Influence of magnetic electrodes thicknesses on the transport properties of magnetic tunnel junctions with perpendicular anisotropy

Léa Cuchet, Bernard Rodmacq, Stéphane Auffret, Ricardo Sousa, Bernard Dieny

Applied Physics Letters

Influence of magnetic electrodes thicknesses on the transport properties of magnetic tunnel junctions with perpendicular anisotropy

Cite as: Appl. Phys. Lett. **105**, 052408 (2014); https://doi.org/10.1063/1.4892450
Submitted: 11 March 2014 . Accepted: 26 July 2014 . Published Online: 06 August 2014

Léa Cuchet, Bernard Rodmacq, Stéphane Auffret, Ricardo C. Sousa, and Bernard Dieny

Influence of magnetic electrodes thicknesses on the transport properties of magnetic tunnel junctions with perpendicular anisotropy

Léa Cuchet, Bernard Rodmacq, Stéphane Auffret, Ricardo C. Sousa, and Bernard Dieny
SPINTEC, UMR 8191, CEA-INAC/CNRS/UJF-Grenoble 1/Grenoble-INP, 38054 Grenoble Cedex, France

(Received 11 March 2014; accepted 26 July 2014; published online 6 August 2014)

The influence of the bottom and top magnetic electrodes thicknesses on both perpendicular anisotropy and transport properties is studied in (Co/Pt)/Ta/CoFeB/MgO/FeCoB/Ta magnetic tunnel junctions. By carefully investigating the relative magnetic moment of the two electrodes as a function of their thicknesses, we identify and quantify the presence of magnetically dead layers, likely localized at the interfaces with Ta, that is, 0.33 nm for the bottom electrode and 0.60 nm for the top one. Critical thicknesses (spin-reorientation transitions) are determined as 1.60 and 1.65 nm for bottom and top electrodes, respectively. The tunnel magnetoresistance ratio reaches its maximum value, as soon as both effective (corrected from dead layer) electrode thicknesses exceed 0.6 nm. © *2014 AIP Publishing LLC*. [http://dx.doi.org/10.1063/1.4892450]

Magnetic Random Access Memories (MRAM) based on Magnetic Tunnel Junctions (MTJs) are promising devices as they combine several advantages: non-volatility, high write speed of a few ns, density ($\sim 6F^2$), infinite endurance ($>10^{16}$ write cycles), and radiation hardness. In recent years, research mainly focused on MTJs with perpendicular magnetic anisotropy (PMA), since, compared to their in-plane counterparts, they provide better thermal stability, lower current densities for spin transfer torque (STT) switching for a given memory retention time[1] and higher storage densities. Standard magnetic junctions are usually composed of a MgO barrier separating two CoFeB layers, an as-deposited amorphous alloy that has the advantage of giving a large tunnel magnetoresistance (TMR) effect after crystallization in the bcc (100) structure compatible with the texture of the MgO barrier, leading to strong spin filtering effects.[2]

To introduce PMA in such structures, it is possible to use the properties of Co/Pt or Co/Pd multilayers.[3,4] These materials indeed provide large PMA (of the order of 1.2 erg/cm^2 for Co/Pt interfaces), thanks to their large spin-orbit coupling, but also induce a strong Gilbert damping which is detrimental for spin transfer torque switching. Therefore, using these materials is adequate for the hard reference layer in STT-RAM but not for the soft storage layer. Large perpendicular interfacial anisotropy has been evidenced at metal/oxide interfaces[5,6] even when the involved materials have weak spin-orbit coupling as in the case of FeCoB/MgO interfaces. This allows getting simultaneously large PMA and weak Gilbert damping which is of crucial interest for the storage layer in scalable STT-RAM. This anisotropy at metal/oxide interface has been shown to be very sensitive to the oxygen and boron content along the MgO interface.[7] Therefore, the oxidation and annealing conditions, as well as the nature of the layers which control the boron diffusion out of the amorphous CoFeB layer upon crystallization, play an important role.[3,8]

In this study, we investigate the effect of varying the thicknesses of the bottom and top magnetic electrodes in perpendicular magnetic tunnel junctions, in order to determine their respective critical thicknesses (transition from out-of-plane to in-plane orientation), their magnetically dead layer thicknesses, as well as the influence of magnetic layer thicknesses on their tunnel transport properties.

Samples were deposited by magnetron sputtering, under an Ar pressure of 2×10^{-3} millibar. The typical stack of the junctions is the following:

Substrate/Ta3/Pt5/$(Co0.5/Pt0.25)_5$/Co0.5/Ru0.9/$(Co0.5/Pt0.25)_3$/Co0.5/Ta0.3/CoFeB/MgO/FeCoB/Ta1/Pt2 (all thicknesses given in nm), where CoFeB stands for a Co-rich alloy ($Co_{60}Fe_{20}B_{20}$) while FeCoB for a Fe-rich one ($Fe_{72}Co_8B_{20}$). Substrate denotes $Si/SiO_2$50/Ta3/CuN60, in order to allow transport measurements. The bottom hard electrode is a synthetic (Co/Pt) antiferromagnet (SAF) coupled to the CoFeB layer through a thin (0.3 nm) Ta spacer. This thin nanocrystallized Ta layer allows a structural transition between the Pt/Co upper part of the SAF (3-fold symmetry fcc structure) and the CoFeB layer (4-fold symmetry bcc structure in contact with the MgO barrier) in order to get a high TMR signal, still keeping a strong magnetic coupling between both Co and CoFeB layers.[9,10] The use of Co/Pt multilayers allows getting strong perpendicular anisotropy, due to their interfacial anisotropy properties.[11]

The storage layer is the top FeCoB electrode, and the MgO tunnel barrier is obtained by natural oxidation of a 1.4 nm thick Mg metallic layer. All deposition rates are of the order of 0.05 nm/s, leading to a negligible uncertainty on the CoFeB and FeCoB thicknesses (deposition times for individual layers varying between about 10 to 30 s, depending on their thickness). The CoFeB and FeCoB thicknesses are varied independently (the bottom CoFeB thickness is kept at 1.2 nm while the top FeCoB thickness varies between 0.8 and 1.8 nm, and the top FeCoB thickness is kept at 1.5 nm while the bottom CoFeB thickness varies between 0.5 and 2.0 nm). Samples were then vacuum-annealed (10^{-6} millibar) for 1 h at 300 °C with no external magnetic field.

From the magnetic cycles measured by Vibrating Sample Magnetometry (VSM), a technique which cannot in general give absolute magnetization values, we extract the relative contributions of the different magnetic layers per unit area. Denoting them by M_1, M_2, and M_3 (M_1/Ru/M_2/

MgO/M_3), there are always two constant contributions when varying the CoFeB or FeCoB thicknesses, and these constant contributions can be used for normalization.

To relate magnetic to transport properties in our junctions, the Current In-Plane Tunneling technique (CIPT) is used, which allows measuring tunnel magnetoresistance on full-sheet samples without any patterning.[12] For such measurements, the resistances of the bottom and top electrodes must be adapted to the RA (resistance-area) product of the MgO barrier, of the order of 30 $\Omega\ \mu m^2$ in our case. Samples are thus deposited on a 60 nm thick CuN buffer layer and covered by a 30 nm thick Ru layer.

Magnetic cycles measured with a perpendicular field by VSM for varying CoFeB and FeCoB thicknesses are presented in Figure 1. Coming from positive field saturation, the high-field transition corresponds to the magnetization reversal of the top PtCo/CoFeB part of the SAF hard electrode, that is to say M2. This can be inferred from the increase of its relative contribution as the bottom CoFeB thickness increases (left curves). Indeed, in the normalized cycles presented in Figure 1, the amplitude of the signal at zero field keeps decreasing as the CoFeB thickness increases. Besides, this is also confirmed by transport measurements, since the high-resistance state is measured for positive applied fields, indicating that the bottom CoFeB electrode is antiparallel to the top FeCoB soft layer. The central transition corresponds to the reversal of the top FeCoB free layer (M3), and the last transition, corresponding to the largest coercive field, represents the hardest part of the SAF M1. The magnetic coupling through the MgO barrier is antiparallel, as usually observed in perpendicular junctions,[10,13] and amounts here to about −50 Oe, without any significant or systematic variation as a function of electrode thicknesses. This antiferromagnetic coupling manifests itself by a shift towards negative fields of the minor loop performed on the free layer (central part of the magnetic cycles, not shown in Figure 1) since, still coming from positive fields, the magnetic layer M2 on the other side of the MgO barrier is already in the "down" direction. M3 thus tends to stay in the "up" direction even if the applied magnetic field turns negative.

For bottom CoFeB thicknesses of 0.8, 1.0, or 1.2 nm, a perfectly horizontal magnetic signal is measured between sharp transitions, reflecting that the anisotropy is perpendicular in the whole structure (Figure 1, left). In contrast, a magnetically hard signal appears for a thickness of 1.6 nm. This signal is not symmetrical with respect to the applied field, which means that it originates from the SAF electrode. This indicates that the magnetization of the upper part of the SAF (M2) starts to tilt away from the perpendicular direction. Decreasing the applied field thus progressively stabilizes M2

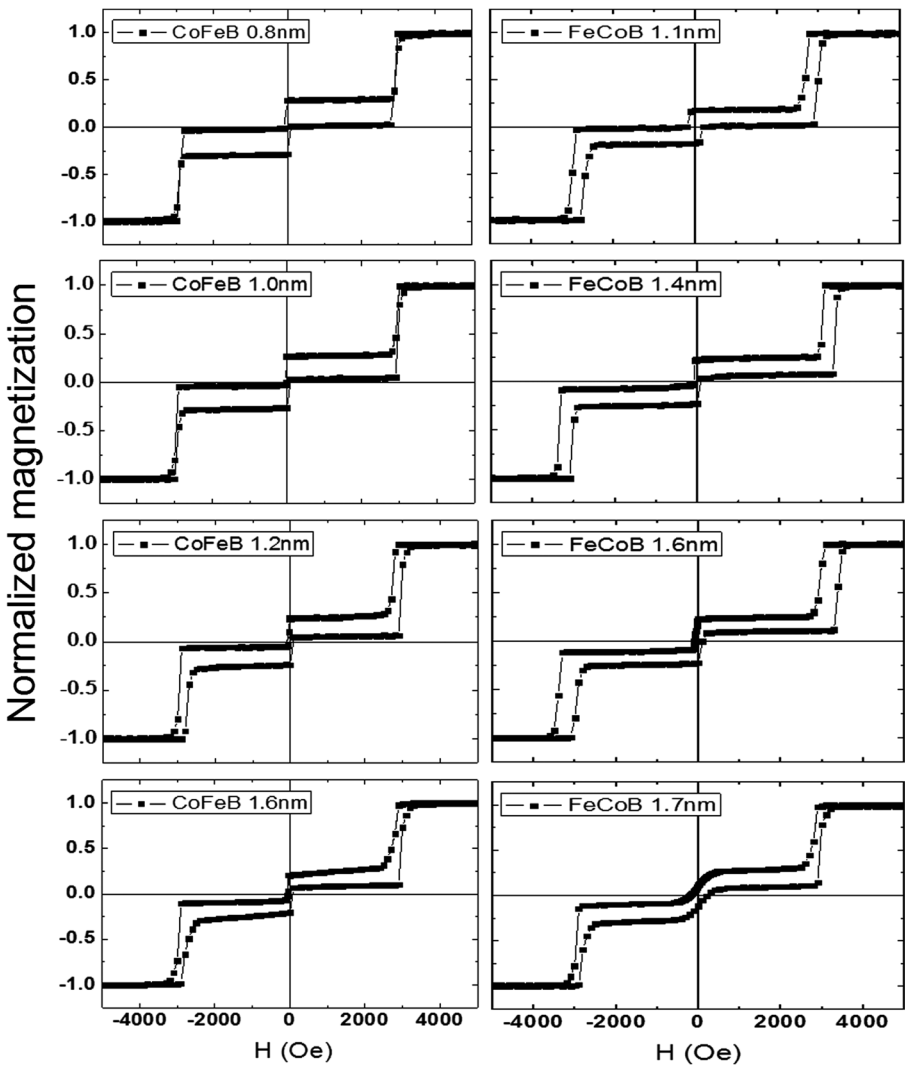

FIG. 1. Magnetic cycles measured by VSM with a perpendicular field for varying thicknesses of bottom CoFeB (left) and top FeCoB (right) electrodes, keeping thicknesses of 1.5 nm for the top FeCoB layer thickness and 1.2 nm for the bottom CoFeB layer one, respectively.

in the perpendicular negative direction, explaining why no slope is observed in negative applied field. When the thickness of the top FeCoB layer increases (Figure 1, right), the easy magnetization axis of the soft layer goes from perpendicular-to-plane to in-plane, a characteristic hard-axis behavior being visible for a thickness of 1.7 nm. Although it is not possible to accurately determine the critical thickness (out-of-plane to in-plane reorientation) of the bottom CoFeB electrode (of the order of 1.6 nm), the measurement of the variation of the anisotropy field with the thickness of the top FeCoB electrode in the vicinity of the reorientation transition leads to a critical thickness of 1.65 nm.

Reminding that our structures can be schematically represented as $M_1/Ru/M_2/MgO/M_3$, we present in Figure 2 the variations of M_2/M_1 as a function of the bottom CoFeB thickness and M_3/M_1 as a function of the top FeCoB thickness.

The M_2/M_1 ratio can be expressed as

$$M_2/M_1 = (4t_{Co}Ms_{Co} + (t_{CoFeB} - t_d)Ms_{CoFeB}))/(6t_{Co}Ms_{Co}),$$

t_{Co} being the thickness of the Co layers in the Pt/Co multilayers, t_d the magnetic dead layer thickness of the CoFeB layer, and Ms the saturation magnetizations of the Co or CoFeB layers. From Figure 2(a), we extract a magnetically dead layer thickness t_d of 0.33 ± 0.02 nm for the bottom CoFeB layer, which corresponds to the intercept between the linear fit and the theoretical ratio M_2/M_1 without any CoFeB contribution, that is, 2/3. This treatment assumes that all ten individual Co layers in both bottom and top (Co/Pt) multilayers have the same saturation magnetizations, despite different interfaces for a few of them (Co/Ru, Ru/Co, and Co/Ta).

This magnetically dead layer of 0.33 nm is probably located at the bottom interface with the Ta insertion layer. Knowing that M_1 is composed of 6 Co layers 0.5 nm thick each, with a saturation magnetization $Ms_{Co} = 1200$ emu.cm^{-3},[14] that is, 15% smaller than the bulk Co value due to Co-Pt interdiffusion, the fitted slope gives a saturation magnetization of the bottom CoFeB layer Ms_{CoFeB} of 600 ± 30 emu.cm^{-3}. One can note that a similar magnetically dead layer thickness is obtained for junctions where the bottom magnetic layer is made of an Fe-rich FeCoB alloy instead of a Co-rich CoFeB one (curves not shown), indicating that it does not depend on the Co/Fe atomic ratio of the electrode.

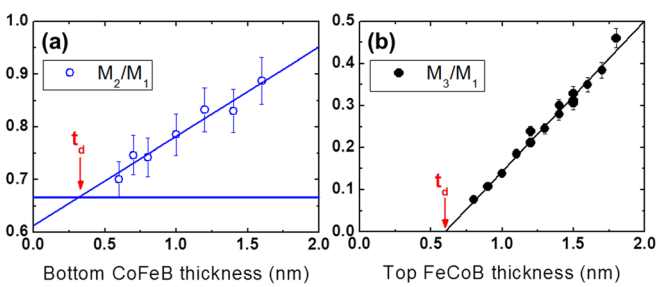

FIG. 2. Magnetization ratio as a function of the bottom CoFeB (a) and top FeCoB (b) thicknesses. The horizontal line in the left figure corresponds to the magnetization ratio M_2/M_1 for zero CoFeB thickness, that is to say, 2/3. Error bars correspond to a 5% uncertainty on the VSM measurements.

A similar data treatment for the top FeCoB layer can be performed, using this time the M_3/M_1 ratio

$$M_3/M_1 = (t_{FeCoB} - t_d)Ms_{FeCoB}/(6t_{Co}Ms_{Co}).$$

In this case (Figure 2(b)), the magnetically dead layer thickness t_d of the upper FeCoB electrode amounts to 0.60 ± 0.04 nm, with a saturation magnetization Ms_{FeCoB} of 1300 ± 60 emu.cm^{-3}. This magnetically dead layer thickness, probably now located at the top FeCoB/Ta interface, is larger than the one obtained for the bottom CoFeB electrode, and may result from the thicker (1.0 nm) Ta capping layer, compared to the 0.3 nm Ta insertion layer on which the bottom CoFeB layer grows. For both Fe-rich and Co-rich electrodes, saturation magnetizations qualitatively agree with those quoted in the literature,[3,7] which however show a rather large scatter. Such a scatter can be attributed to the strong dependence of saturation magnetization on annealing conditions[15] resulting from varying residual boron concentrations.

In order to check the validity of our treatment, we present in Figure 3 the variation of the ratio M_3/M_1 (for varying M_2) and M_2/M_1 (for varying M_3) as a function of bottom and top electrodes thicknesses, respectively. These ratios are found reasonably constant and equal to the theoretical ones (0.32 ± 0.03) for M_3/M_1 and 0.81 ± 0.08 for M_2/M_1). These expected values are calculated using the saturation magnetizations and the bottom and top magnetically dead layers mentioned above.

We do not try in this Letter to extract from the present measurements values of interface and volume anisotropy energies, as is usually done in the recent literature,[3,9,15–19] by plotting the effective anisotropy energy ($K_{eff} = H_{an}Ms/2$, where H_{an} is the anisotropy field and Ms the saturation magnetization) times magnetic thickness as a function of magnetic thickness, and extracting volume and interface terms from the slope and zero intercept of such an ideally linear plot.[11] The reason is that anisotropy fields of both bottom and top electrodes are not different enough (especially for small thicknesses) to be determined independently in such junctions. A solution would be to study single electrodes, or junctions in which one of the bottom or top electrode is rendered non-magnetic, by using CoFeB or FeCoB layers on the

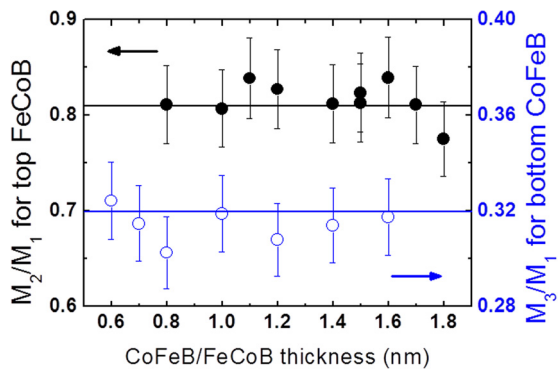

FIG. 3. Magnetization ratio of the constant magnetic contributions M2/M1 as a function of top FeCoB thickness, filled black circles, left-hand scale, and M3/M1 as a function of bottom CoFeB thickness, open blue circles, right-hand scale. Horizontal lines correspond to the theoretical values, 0.81 and 0.32, respectively.

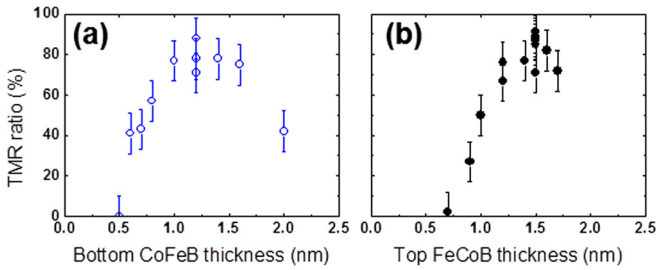

FIG. 4. TMR ratio as a function of bottom CoFeB (a) and top FeCoB (b) thicknesses.

other side of the MgO barrier with a thickness smaller than their dead layer ones. One should assume in this case that such modifications do not have any impact on the growth-induced properties of the rest of the structure. However, we often observed different anisotropy properties in single electrodes, compared to junctions in which one of the magnetic electrodes is rendered non-magnetic, or to full junctions. An explanation could be that, since boron atoms migrate out of the CoFeB layer upon annealing, varying the magnetic thickness could modify the amount of boron atoms at the oxide and cap (seed) interfaces,[7] having consequences on their anisotropy properties.

We now correlate magnetic and transport properties by measuring the tunnel magnetoresistance of full-sheet samples with the Current In-Plane Tunneling (CIPT) technique. Figure 4(a) shows that, as the thickness of the bottom CoFeB electrode increases, the TMR ratio increases to about 90% for thicknesses between 1.0 and 1.6 nm, followed by a decrease when a low-field slope appears in the M(H) curves. This slope is attributed to a progressive tilt of the magnetization of the upper part of the SAF (denoted as M_2) away from the perpendicular direction, as indicated by the magnetic cycles of Figure 1 (left). Perfect parallel and antiparallel states can, thus, not be reached anymore, leading to an artificial decrease of the TMR ratio. Similarly, samples with varying top FeCoB thickness (Figure 4(b)) show an increase of TMR with FeCoB thickness, with an asymptotic value between 1.2 and 1.7 nm. The maximum TMR value is not obtained at the same thickness for both electrodes, due to the fact that their respective dead layers thicknesses differ.

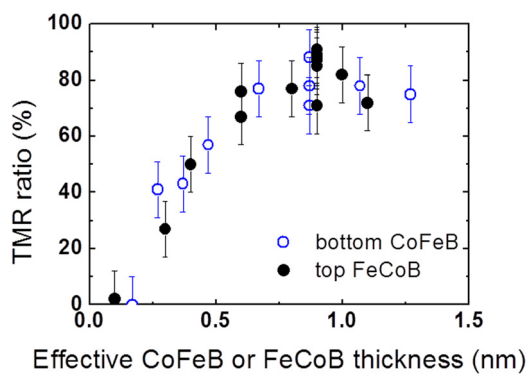

FIG. 5. TMR ratio as a function of bottom CoFeB (blue open circles) and top FeCoB (black filled circles) thicknesses, respectively, after substraction of their corresponding dead layer thicknesses.

A plot of the TMR ratio as a function of the effective magnetic thickness, i.e., correcting the nominal values from their dead layers contributions, gives identical thickness dependences, as can be seen on Figure 5. The TMR ratio starts increasing as soon as the effective magnetic thickness reaches 0.3 nm. One can also note that the measured RA product of our junctions is essentially constant at about 30 Ω μm^2 on both CoFeB and FeCoB thickness ranges, showing that the TMR decrease for small magnetic thicknesses is not linked to some deterioration of the quality of the MgO barrier, but rather to a progressive decrease of the electron polarization through thinner magnetic electrodes.

Finally, one can note that the maximum TMR value (90%) obtained in these perpendicular junctions prepared in our sputtering tool is slightly lower than the one obtained in corresponding in-plane top-pinned junctions, with a TMR of the order of 120% (unpublished). This difference can result from a deterioration of the quality of the MgO barrier due to the (Co/Pt) multilayer SAF structure on which it grows, possibly leading to some increased roughness of the barrier. This could be related to the slightly larger RA product we measure on perpendicular junctions compared to in-plane ones, which give a RA product around 20 Ω μm^2.

In conclusion, the influence of magnetic thicknesses of bottom CoFeB and top FeCoB electrodes of perpendicular tunnel junctions on their tunnel transport properties was studied. Quantitative analysis of relative magnetization measurements indicates that dead layers exist in the bottom and top magnetic electrodes, probably located at the bottom Ta/CoFeB and top FeCoB/Ta interfaces, with respective thicknesses of 0.33 nm for the bottom electrode and 0.60 nm for the top one. Critical thicknesses, i.e., transitions from out-of-plane to in-plane orientation of the magnetization, are found equal to 1.60 nm for the bottom CoFeB layer and 1.65 nm for the top FeCoB one. In the thickness range where both top and bottom magnetizations are out-of-plane, or can be brought out-of-plane thanks to the applied field, we observe a similar thickness dependence on effective magnetic thickness (i.e., corrected from magnetically dead layer thickness) of the TMR ratio for both electrodes. For both bottom and top magnetic thicknesses, the TMR ratio saturates to a value of about 90% as soon as both effective magnetic thicknesses reach 0.6 nm.

This work benefited from financial support of the ANR (French National Research Agency) under project ANR-NANO PATHOS and of the European Union under ERC HYMAGINE Project No. 246942. CIPT measurements were carried out at Crocus Technology.

[1]O. G. Heinonen and D. V. Dimitrov, J. Appl. Phys. **108**, 014305 (2010).
[2]D. D. Djayaprawira, K. Tsunekawa, M. Nagai, H. Maehara, S. Yagamata, N. Watanabe, S. Yuasa, and K. Ando, Appl. Phys. Lett. **86**, 092502 (2005).
[3]D. C. Worledge, G. Hu, D. W. Abraham, J. Z. Sun, P. L. Trouilloud, J. Nowak, S. Brown, M. C. Gaidis, E. J. O'Sullivan, and R. P. Robertazzi, Appl. Phys. Lett. **98**, 022501 (2011).
[4]K. Mizunuma, M. Yamanouchi, S. Ikeda, H. Sato, H. Yamamoto, H.-D. Gan, K. Miura, J. Hayakawa, F. Matsukura, and H. Ohno, Appl. Phys. Express **4**, 023002 (2011).
[5]S. Monso, B. Rodmacq, S. Auffret, G. Casali, F. Fettar, B. Gilles, B. Dieny, and P. Boyer, Appl. Phys. Lett. **80**, 4157–4159 (2002).

[6]B. Rodmacq, A. Manchon, C. Ducruet, S. Auffret, and B. Dieny, Phys. Rev. B **79**, 024423 (2009).
[7]S. Ikeda, R. Koizumi, H. Sato, M. Yamanouchi, K. Miura, K. Mizunuma, H.-D. Gan, F. Matsukura, and H. Ohno, IEEE Trans. Magn. **48**, 3829–3832 (2012).
[8]H. Yamamoto, J. Hayakawa, K. Miura, K. Ito, H. Matsuoka, S. Ikeda, and H. Ohno, Appl. Phys. Express **5**, 053002 (2012).
[9]V. Sokalski, M. T. Moneck, E. Yang, and J.-G. Zhu, Appl. Phys. Lett. **101**, 072411 (2012).
[10]L. Cuchet, B. Rodmacq, S. Auffret, R. C. Sousa, C. Ducruet, and B. Dieny, Appl. Phys. Lett. **103**, 052402 (2013).
[11]M. T. Johnson, P. J. H. Bloemen, F. J. A. den Broeder, and J. J. de Vries, Rep. Prog. Phys. **59**, 1409–1458 (1996).
[12]D. C. Worledge and P. L. Trouilloud, Appl. Phys. Lett. **83**, 84–86 (2003).
[13]L. E. Nistor, B. Rodmacq, S. Auffret, A. Schuhl, M. Chshiev, and B. Dieny, Phys. Rev. B **81**, 220407 (2010).
[14]S. Bandiera, R. C. Sousa, Y. Dahmane, C. Ducruet, C. Portemont, V. Baltz, S. Auffret, I. L. Prejbeanu, and B. Dieny, IEEE Magn. Lett. **1**, 3000204 (2010).
[15]A. Natarajarathinam, Z. R. Tadisina, T. Mewes, S. Watts, E. Chen, and S. Gupta, J. Appl. Phys. **112**, 053909 (2012).
[16]T. Liu, J. W. Cai, and Li Sun, AIP Adv. **2**, 032151 (2012).
[17]V. B. Naik, H. Meng, and R. Sbiaa, AIP Adv. **2**, 042182 (2012).
[18]J. Sinha, M. Hayashi, A. J. Kellock, S. Fukami, M. Yamanouchi, H. Sato, S. Ikeda, S. Mitani, S.-H. Yang, S. S. P. Parkin, and H. Ohno, Appl. Phys. Lett. **102**, 242405 (2013).
[19]V. Sokalski, D. M. Bromberg, M. T. Moneck, E. Yang, and J.-G. Zhu, IEEE Trans. Magn. **49**, 4383–4385 (2013).